ARTICLES

Thiol-Derivatized Nanocrystalline Arrays of Gold, Silver, and Platinum

K. Vijaya Sarathy, Gargi Raina, R. T. Yadav, G. U. Kulkarni, and C. N. R. Rao*

Chemistry and Physics of Materials Unit, Jawaharlal Nehru Centre for Advanced Scientific Research, Jakkur, Bangalore-560064, India

Received: May 7, 1997; In Final Form: July 16, 1997[⊗]

A simple procedure has been developed to prepare thiol-derivatized nanoparticles of metals. The procedure involves the transfer of well-characterized metal hydrosols to a hydrocarbon medium containing the thiol. Thiol-derivatized nanoparticles Au, Ag, and Pt of near spherical shape forming nanocrystalline arrays have been characterized by X-ray diffraction, transmission electron microscopy (TEM), and other techniques. Thiol-derivatized Au particles of mean diameters of 1.0, 2.1, and 4.2 nm from nanocrystalline arrays show characteristic X-ray diffraction patterns. The nanoparticles exhibit Moiré fringes when deposited on a flake of $MoSe_2$, showing that each particle is in itself crystalline. Besides spherical nanoparticles, thiol-derivatized particles of other shapes have been prepared, hexagonal Pt nanoparticles being particularly novel. Scanning tunneling microscopy images not only confirm the size and shape of nanoparticles revealed by TEM, but also show evidence for thiol molecules on the surface.

Introduction

Nanoparticles of gold and other noble metals are of great interest today because of their interesting optical, electrical, and other properties and possible applications in microelectronics.[1−3] Chemical methods for the preparation of colloidal metal sols have been described in the literature.[3−5] The methods involve the reduction of the relevant metal salt in the presence of a suitable surfactant, the surfactant being useful in controlling the growth of the metal particles. Metal nanoparticles, particularly those stabilized by alkane thiols, are known to self-assemble into cross-linked structures or nanocrystalline arrays on removal of the solvent.[6−8] The procedure employed to prepare thiol-passivated nanoparticles involves the extraction of the metal ions from an aqueous medium to a hydrocarbon layer by means of a phase-transfer reagent such as tetraoctylammonium bromide and then to carry out the reduction with $NaBH_4$ in the presence of an alkane thiol.[9,10] In this procedure, the attachment of the thiol molecules to the metal nanoparticles occurs concomitantly with the formation of the particles and allows little control over their shapes. It is therefore desirable to have a procedure where metal nanoparticles themselves, rather than the ions, are phase-transferred for thiol passivation.

The present study is concerned with developing a simple procedure wherein metal nanoparticles of desired shape and size distribution in a hydrosol are readily transferred to a nonpolar medium containing an alkane thiol to obtain thiol-derivatized particles ensuring a careful replacement of the surfactant layer. The method is different from that of Weisbecker et al.[11] who obtained self-assembled monolayers on gold colloids in 50% aqueous ethanol in the presence of alkanethiols. By employing such a procedure, we have prepared thiol-derivatized Au nanoparticles of different sizes and shapes and examined them by transmission electron microscopy (TEM) and scanning tunneling microscopy (STM), besides characterizing the surfaces of the nanoparticles by various spectroscopic techniques. The thiol-passivated metal particles formed in this manner are found to form nanocrystalline arrays on solid substrates giving characteristic X-ray diffraction patterns. We have examined the crystallinity of the nanoparticles in such arrays by recording the Moiré patterns of the particles deposited on a flake of $MoSe_2$. We have extended the present method of preparation of thiol-derivatized Au nanoparticles to the preparation of spherical, thiol-derivatized particles of silver as well as platinum, the latter for the first time. In addition, we have prepared thiol-passivated particles of hexagonal shape.

Experimental Section

Thiol-derivatized nanoparticles of Au were first prepared starting with the hydrosol. The hydrosol containing nanoparticles of Au was prepared by the reduction of 2.0 mL of a solution of $HAuCl_4$ solution (25 mM) using partially hydrolyzed tetrakis(hydroxymethyl) phosphonium chloride (THPC) as the reducing agent,[12] having prepared the reagent by the addition of 1 mL of a fresh solution of THPC (50 mM) in water to 47 mL of 6.38 mM NaOH solution. To the dark brown Au sol obtained 100 mL of a 0.25 mM solution of dodecanethiol in toluene (Au:S = 2:1) was added to obtain immiscible layers consisting of the transparent organic phase containing the thiol on the top and the colored hydrosol at the bottom. To this biphasic mixture, 125 mL of concentrated HCl was added under stirring. This resulted in a remarkably swift movement (within 3 min) of the Au nanoparticles to the hydrocarbon layer containing the thiol. Clearly, the gold particles have an inherent attraction to the thiol molecules. This could be seen vividly by the complete transfer of color across the interface as shown in Figure 1. The gold sol in toluene was shaken with water several times to remove traces of HCl and evaporated to around 2 mL in a rotary evaporator. The excess thiol was removed by the addition of 350 mL of ethanol (95%). The dark brown solid thus obtained was filtered, washed with ethanol, and dispersed in 10 mL of toluene. In order to prepare Au particles of different

[⊗] Abstract published in *Advance ACS Abstracts,* October 15, 1997.

S1089-5647(97)01544-7 CCC: $14.00

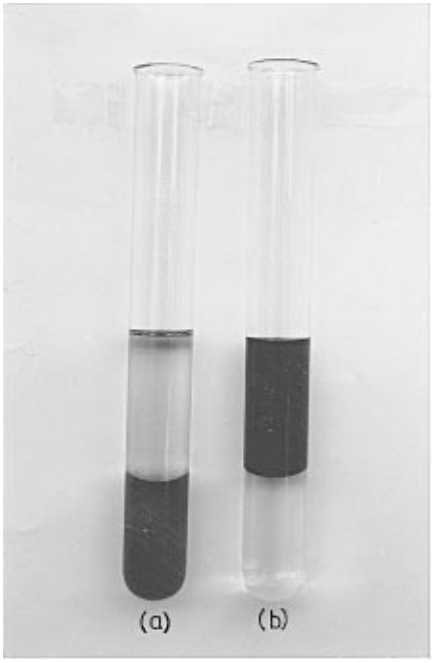

Figure 1. Immiscible layers of (a) the gold hydrosol (at the bottom) and the clean toluene solution containing the thiol (on top). (b) Thiol-derivatized Au sol in toluene (on top) and the clean aqueous solution at the bottom.

sizes, the above procedure was repeated with hydrosols obtained using different amounts of $HAuCl_4$ solution. The color of the hydrosol and also that of the toluene sol varied from light brown to reddish brown as the initial amount of $HAuCl_4$ solution was increased from 1.8 to 2.2 mL.

Hydrosols containing nanoparticles of Ag and Pt were prepared by the use of $NaBH_4$ as the reducing agent. A 0.01 M solution of $NaBH_4$ aged for 3 h was added dropwise up to 0.5 mL to a beaker containing 100 mL of the stock solution of 0.29 mM $AgNO_3$ or 2.6 mM H_2PtCl_6 under vigorous stirring. The Ag solution turned light yellow and that of Pt became yellowish grey due to formation of metal sols. To these hydrosols was added 20 mL of the 1.668 mM dodecanethiol solution resulting in a biphasic mixture. Around 1.0 mL of concentrated HCl was added dropwise under stirring to the mixture resulting in the transfer of the nanoparticles to the toluene layer, as evidenced by the color change. No special precaution to maintain oxygen free atmosphere seemed necessary.

We have also thiol-derivatized silver nanoparticles, which were initially coated with poly(vinylpyrrolidone) (PVP).[4] To a 20 mL of bright yellow Ag−PVP sol in a separating funnel was added 10 mL of the 1.668 mM thiol solution in toluene. To this resulting medium, a fresh aqueous solution of $NaBH_4$ (0.01 M) was added in excess. A thin yellow layer of the thiol-derivatized Ag sol formed on the turbid solution. The bottom layer was drained out, and the yellow layer was repeatedly washed with the $NaBH_4$ solution.

In a recent report in the literature,[5] the preparation of regular cubic Pt nanoparticles using sodium polyacrylate as a stabilizing agent has been described. We have adopted a variant of this procedure to prepare hexagonal nanoparticles of platinum. In our procedure, 2.1 mg of K_2PtCl_6 was dissolved in 50 mL of water containing 8.4 mg of sodium polyacrylate (MW 2100, Aldrich). Pure argon was bubbled through this solution for 20 min, followed by H_2 gas for 5 min. The glass vessel was sealed and left undisturbed for 12−14 h. The resulting light-golden Pt sol was mixed with 20 mL of 1.668 mM toluene solution of the thiol to yield a milky solution. To this solution, 0.01 M $NaBH_4$ solution was added dropwise followed by vigorous shaking, to obtain a thin yellow layer containing thiol-derivatized Pt nanoparticles floating above the milky layer. The sol was washed with an excess of $NaBH_4$ solution.

Thiol-derivatized metal nanoparticles were characterized by several techniques. X-ray diffraction (XRD) patterns of the films of the thiol-derivatized metal particles obtained by vacuum drying of the concentrated toluene sols on glass substrates were recorded with a Seifert 3000TT instrument using Cu Kα. Transmission electron microscopy (TEM) images were recorded with a JEOL-3010 microscope operating at 300 KeV. For this purpose, samples were prepared by placing a drop of the sol containing thiol-derivatized metal nanoparticles on a holey carbon grid (dia-3 mm). The solvent was evaporated before introducing the grid into the microscope. Histograms of particle size distributions were obtained using Quantimat image analyser. X-ray photoelectron spectroscopic (XPS) measurements were carried out using ESCALAB MKIV (VG Scientific) instrument. A few drops of the toluene containing thiol-derivatized metal nanoparticles was evaporated on amorphized graphite substrate before recording the spectrum. Al Kα (1486.6 eV) radiation was used as the source. Ultraviolet−visible absorption spectroscopic measurements of the thiol coated metal sols were carried out on a Pye-Unicam SP8-100 spectrophotometer in the double-beam mode between 800−300 nm in 1 cm quartz curvettes. Scanning tunneling microscopy (STM) images were recorded with a Nanoscope (II) of Digital Instruments by employing Pt−Ir tips. Samples for STM were prepared by evaporating the sols of the thiol-derivatized metal nanoparticles on freshly cleaved highly oriented pyrolytic graphite (HOPG) surface.

Results and Discussion

The simple procedure of transferring the metal nanoparticles from an aqueous medium to a toluene medium containing the thiol, described in the Experimental Section, has enabled us to obtain thiol-derivatized Au nanoparticles of different size distributions. In Figure 2 we show TEM images of thiol-derivatized Au nanoparticles of three size distributions, prepared from hydrosols containing different concentrations of $HAuCl_4$. The particle size dependence on the concentration of $HAuCl_4$ is evident from the figure. The particles are near spherical and the size distributions are reasonably narrow with the mean diameters of the particle arrays in a, b, and c are 4.2, 2.1, and 1.0 nm respectively.

X-ray photoelectron spectroscopic studies of the thiol-derivatized Au nanoparticles prepared by the THPC reduction, showed the Au($4f_{7/2}$) core-level feature at 84 eV corresponding to Au^0 state. There was a feature at 163.5 eV due to S(2p) showing that the thiol molecules were chemisorbed on the surface of the Au particles. There was no evidence of a feature due to P(2p) from the THPC reagent in the spectrum, unlike particles from the hydrosol which showed a feature at ∼133 eV. A curious feature of the thiol-derivatized Au particles is that the Au($4f_{7/2}$) binding energy was identical to the value of the bulk metal (84 eV), irrespective of the particle size. This is not expected since the core-level binding energy of metals is known to increase with the decrease in particle or cluster size, specially when the diameter is smaller than 2 nm.[13,14] The invariance in binding energy with respect to the bulk metal value found here could either be due to the effect of the thiol molecules or due to the formation of the nanocrystalline arrays shown in Figure 2. In order to test this, we measured the Au(4f) binding energy of gold clusters of various sizes deposited on amorphized

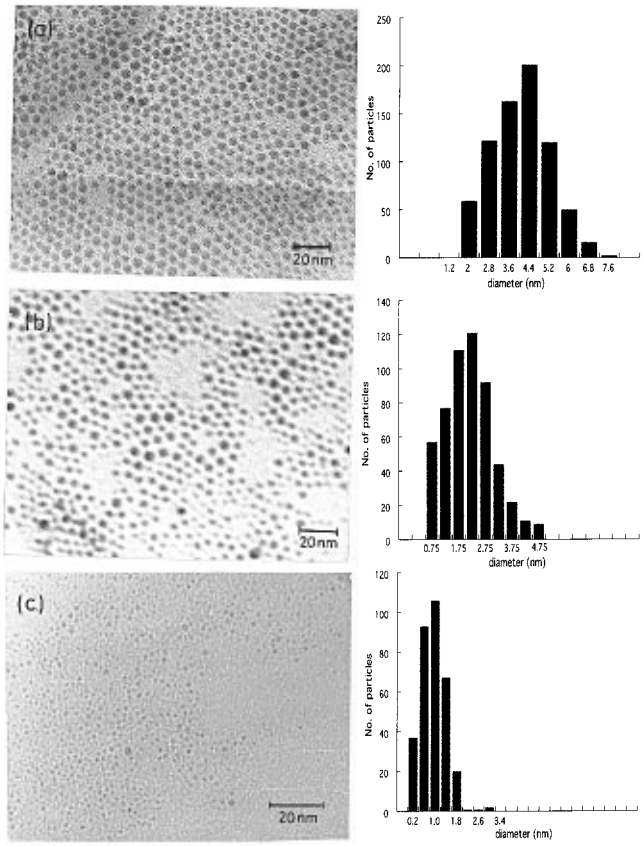

Figure 2. TEM images of the thiol-derivatized Au nanoparticles. The particle size distributions are shown in the form of histograms alongside the TEM images. The nanoparticles in a, b, and c were obtained by using 2.2, 2.0, and 1.8 mL of the 25 mM $HAuCl_4$ solution, respectively.

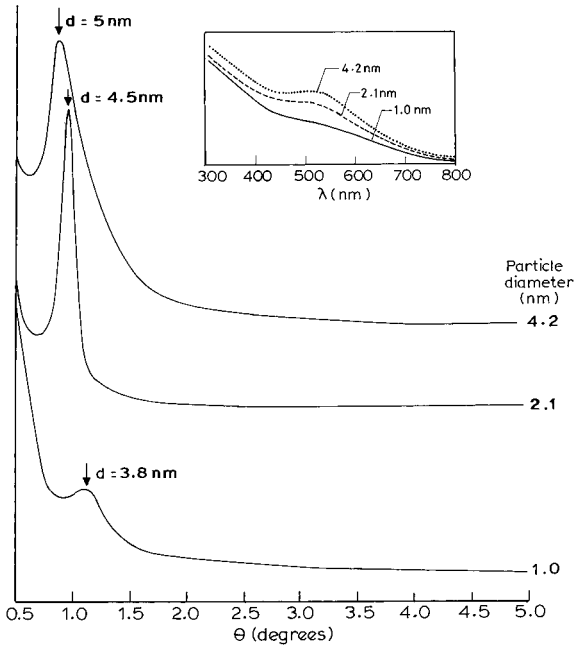

Figure 3. XRD patterns from the nanocrystalline arrays of Au particles of different mean diameters (4.2, 2.1, and 1.0 nm). Inset of the figure displays the UV−vis spectra of these particles.

graphite substrate by the resistive evaporation of gold in the UHV chamber of the electron spectrometer,[13] before and after the passivation of clusters by dodecanethiol. The measurement showed that, in the absence of thiol, gold clusters do indeed show the variation as reported in the literature.[13,14] Upon thiol-derivatization, the binding energy of the Au($4f_{7/2}$) core level of all the clusters is 84(±0.1) eV, irrespective of the particle size.

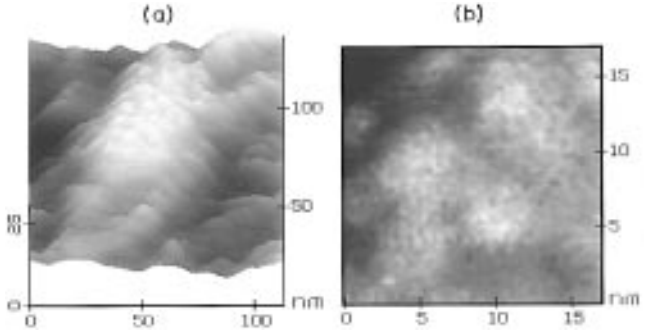

Figure 4. STM images of (a) a portion of a crystallite formed by thiol-derivatized Au nanoparticles of ∼5 nm diameter. (b) Low-scan image of Au nanoparticles of the crystallite in a; we ascribe the several small features seen on each of the particles to the chemisorbed thiol molecules.

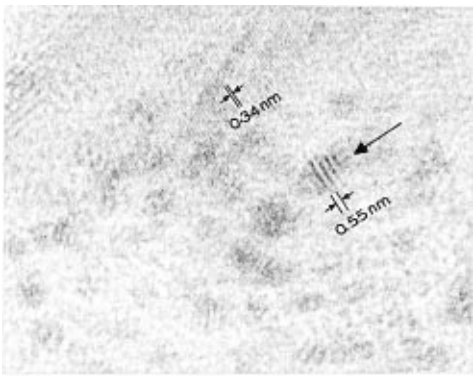

Figure 5. TEM image obtained with Au nanocrystallites deposited on a $MoSe_2$ flake. The prominent fringes (shown by an arrow) with a regular spacing of 0.55 nm are due to Moiré interference.

These experiments suggest that the thiol molecules may donate electrons to the small Au clusters (2 nm diameter) and compensate for the cluster size effect.

The TEM images in Figure 2 reveal that thiol-derivatized particles readily form nanocrystalline arrays over tens of nms with regular spacing (∼1 nm) between the particles. Particles with the mean diameter of 4.2 nm form a close-packed structure, while the smaller particles of mean diameters of 2.1 and 1.0 nm form superstructure islands, with voids in between. All of them, however, show characteristic XRD patterns. In Figure 3, we show the XRD patterns obtained with the nanoparticles with the mean diameters of 4.2, 2.1, and 1.0 nm, giving low-angle peaks corresponding to *d*-spacings of 5.0, 4.5, and 3.8 nm, respectively. These diffraction peaks are likely to result from the nanocrystalline arrays revealed in the TEM images, in particular due to the (110) spacing of the BCC structure.[6] We do not see higher angle peaks due to the limited thickness of the films and also possibly due to the presence of distribution of sizes. Accordingly, the XRD feature is more intense in the case of the bigger nanoparticles and broader in the case of the small 1.0 nm particles. The distance between the nanoparticles deduced from the *d*-spacings is somewhat smaller than the expected value (twice the radius of the particle and the thiol layer thickness). Thus, in the case of the 4.2 nm particles, the *d*-spacing of 5.0 nm gives an inter particle distance of 0.8 nm, which is smaller than the estimated surfactant layer thickness of ∼1.5 nm. It appears that there is a significant overlap (or close-packing) of the passivating layers of the thiol molecules on the neighboring particles.

The UV−vis absorption spectra of the toluene gold sols (see inset of Figure 3) show a distinct plasmon band centered around 525 nm in the case of the 4.2 and 2.1 nm particles, the intensity of the band being higher with the bigger particles. We hardly

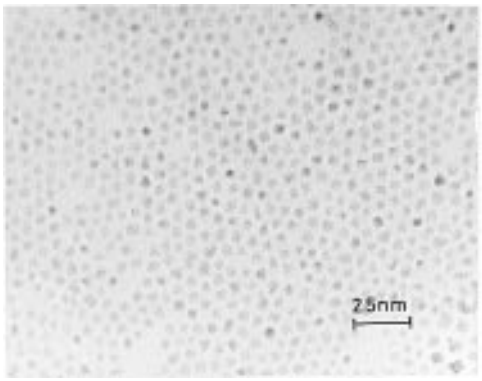

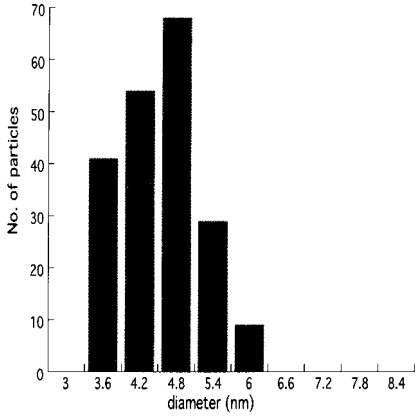

Figure 6. TEM image of the thiol-derivatized Ag particles prepared by $NaBH_4$ reduction. Histogram showing the particle size distribution (mean diameter = 4.2 nm) is also displayed.

see any feature in the 525 nm region in the case of the 1.0 nm particles. Although the presence or absence of a plasmon band does not provide direct information on the electronic structure, it is possible that such small particles are truly not metallic. There is some evidence to show that Au nanoparticles of 1.0 nm diameter or less, prepared by different methods, are nonmetallic.[14]

Scanning tunneling microscopy (STM) images of thiol-derivatized Au nanoparticles of 4.2 nm diameter are shown in Figure 4. The STM image in top view (Figure 4a) shows a large number of particles arranged into a lattice of a crystallite extending over 50 nm. We find that the image yield a diameter of the nanoparticle that is close to the value estimated from the TEM image. The image in a smaller scan shown in Figure 4b provides certain details. On each of the particles, there is a large number of high-contrast features ascribable to the chemisorbed thiol molecules. By counting the features on the corrugated portion, we obtain an average value for the number of thiol molecules on a 4.2 nm diameter particle to be around 250. We obtain a similar estimate of the number of thiol molecules from the relative intensities of the Au($4f_{7/2}$) and S(2p) features in XPS. It may be noted that the thiol coverage obtained by us (~20 $Å^2$/molecule) compares well with the reported value on plane Au surfaces (~21 $Å^2$/molecule).[15]

We have sought to examine the crystallinity of the Au nanoparticles by making use of the Moiré patterns obtained from the nanoparticles on thin flakes of $MoSe_2$. In Figure 5, we show a TEM image collected in a region where the Au nanoparticles showed strong interference with the support lattice of $MoSe_2$. The figure distinctly shows Moiré patterns in the background of the $MoSe_2$ lattice. The Moiré pattern associated with each particle is uniform with a spacing of 0.55 nm, confirming that each of them is a nanocrystallite. The observed lattice spacing

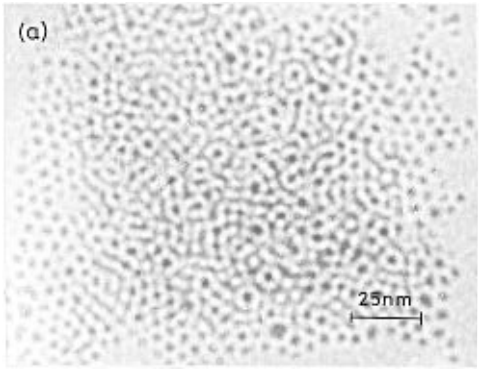

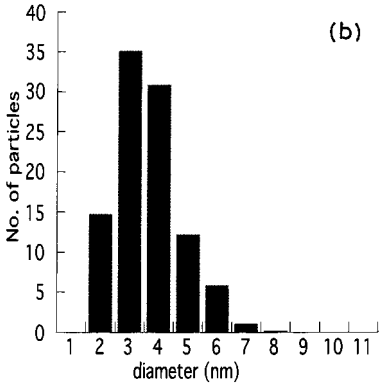

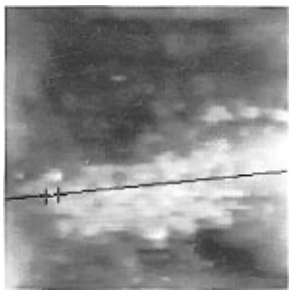

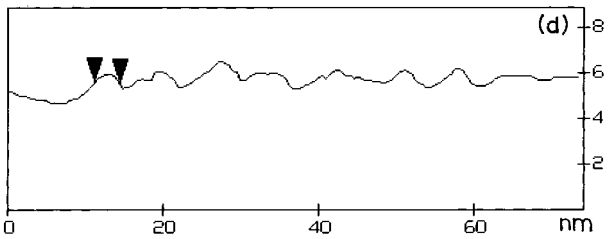

Figure 7. (a) TEM image of thiol-derivatized Pt nanoparticles prepared by $NaBH_4$ reduction. (b) The histogram shows the particle size distribution (mean diameter = 4.1 nm). (c) STM image of a crystallite formed by spherical Pt nanoparticles. (d) The line profile of the crystallite in c with the two arrows marking the diameter of the particle.

of $MoSe_2$ is 0.34 nm corresponding to the (006) planes. It is likely that the diffraction pattern due to Au (111) planes (0.24 nm) of the nanocrystallites (which are faintly visible in some of the particles in Figure 5) interfere with that from the $MoSe_2$ (006) planes to produce the Moiré fringes.[1] For instance, with the particle indicated by an arrow in Figure 5, the angle between the two interfering lattices is around 20°, close to that estimated from the Moiré formula.

In Figure 6, we show the TEM image of the thiol-derivatized Ag nanoparticles obtained by the $NaBH_4$ reduction. The particle shape is not always spherical, but the size distribution is fairly narrow and the mean diameter is 4.2 nm. Here again we see a

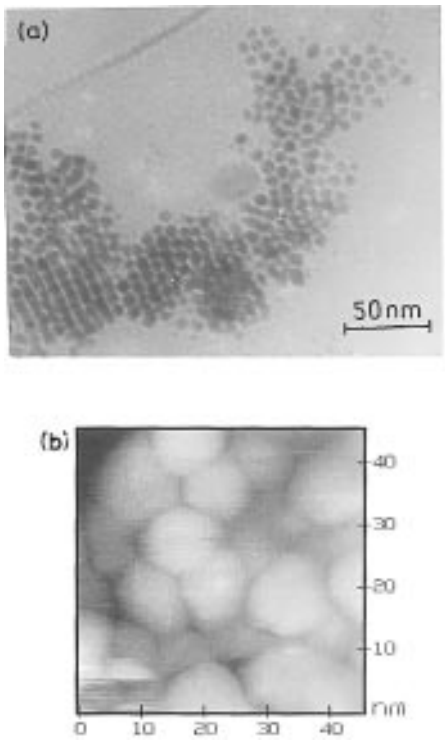

Figure 8. (a) TEM image of thiol-derivatized Pt particles prepared by the sodium polyacrylate method. Hexagonal nanocrystallites forming a honeycomb structure are seen. (b) STM image of hexagonal Pt nanocrystallites. The hexagonal stacking of the three top layers is clearly seen.

nanocrystalline array formed by the particles. Similar nanocrystalline arrays of thiol-derivatized Ag particles have been prepared by vacuum evaporation technique.[8] In Figure 7 we show a TEM image of the thiol-derivatized Pt nanoparticles obtained by $NaBH_4$ reduction. The particles are spherical with a mean diameter of 4.1 nm. There is a clear evidence for the formation of a nanocrystalline array. The STM image of the Pt particles shown in Figure 7 confirms the spherical shapes. The line profile given next to the STM image provides a measure of the particle size, which is comparable to that from TEM.

In Figure 8 we show a TEM image of the Pt nanoparticles obtained by using sodium polyacrylate. We distinctly see that the particles have a hexagonal shape, forming close-packed structures resembling honeycomb pattern, each honeycomb representing a nanoparticle. This is to be contrasted with the spherical shape of the particles in Figure 7 prepared in the absence of sodium polyacrylate. This is the first observation of hexagonal particles of Pt arranged into a nanocrystalline array. The honeycomb structures in Figure 8 have a mean diameter of around 8 nm. The wiggly pattern in the TEM image is due to the second layer of the honeycomb structure sitting over the first layer in a AB-type packing. Particles which are not well formed hexagons are left out in the packing, as evidenced in the image. The STM image (top view) in Figure 8 is consistent with the hexagonal shape. The image shows the well-defined edges of the central nanoparticles. We have not been able to prepare thiol-passivated cubic particles[5] of Pt by the procedure described here.

In conclusion, the present work details an alternative method for thiol-derivatization of metal nanoparticles compared to the method of Brust et al.[9] In our procedure, metal particles of desired shape and size distribution prepared initially in a hydrosol are transferred to an organosol following thiol-derivatization and the end point of the process is marked by the transfer of color between the layers if immiscible solvents like water and toluene are used. This is particularly advantageous since many of the water soluble reagents may be easily washed away. Besides, this method may provide a rather unique way of replacing polymeric or ligand shells surrounding metal nanoparticles by thiol molecules.

Acknowledgment. We thank the Department of Science and Technology, Government of India, for support of this research.

References and Notes

(1) Andres, R. P.; Bielefeld, J. D.; Henderson, J. I.; Janes, D. B.; Kolagunta, V. R.; Kubiak, C. P.; Mahoney, W. J.; Osifchin, R. G. *Science* **1996**, *273*, 1690.

(2) (a) deHeer, W. A. *Rev. Mod. Phys.* **1993**, *65*, 611. (b) Fukumi, K.; Chayahara, A.; Kadono, K.; Sakaguchi, T.; Horino, Y.; Miya, M.; Fujji, K.; Hayakawa, J.; Satou, M. *J. Appl. Phys.* **1994**, *75*, 3075.

(3) Schimd, G. *Chem. Rev.* **1992**, *92*, 1709.

(4) (a) Rao, C. N. R. *Chemical Approaches to the Synthesis of Inorganic Materials*. John Wiley: New York, 1994. (b) Fendler, J. H.; Meldrum, F. C. *Adv. Mater.* **1991**, *7*, 607. (c) Ayyappan, S.; Gopalan, R. S.; Subbanna, G. N.; Rao, C. N. R. *J. Mater. Res.* **1997**, *2*, 398.

(5) Ahmadi, T. S.; Wang, L.; Henglein, A.; El-Sayed, M. A. *Chem. Mater.* **1996**, *8*, 1161.

(6) Whetten, R. L.; Khoury, J. T.; Alvarez, M.; Murthy, S.; Vezmar, I.; Wang, Z. I.; Stevens, P. W.; Cleveland, C. L.; Luedtke, W. D.; Landman, U. *Adv. Mater.* **1996**, *8*, 428.

(7) Badia, A.; Singh, S.; Demers, L.; Cuccia, L.; Brown, R. B.; Lennox, R. B. *Chem. Eur. J.* **1996**, *2*, 359.

(8) Harfenist, S. A.; Wang, Z. L.; Alvarez, M. M.; Vezmar, I.; Whetten, R. L. *J. Phys. Chem.* **1996**, *100*, 13904.

(9) (a) Brust, M.; Walker, M.; Bethel, D.; Schiffrin, D. J.; Whyman, R. *J. Chem. Soc., Chem. Commun.* **1994**, 801. (b) Brust, M.; Bethell, D.; Schiffrin, D. J.; Kiely, C. J. *Adv. Mater.* **1995**, *7*, 795.

(10) Leff, D. V.; Ohara, P. C.; Heath, J. R.; Gelbart, W. M. *J. Phys. Chem.* **1995**, *99*, 7036.

(11) Weisbecker, C. S.; Merritt, M. V.; Whitesides, G. M. *Langmuir* **1996**, *12*, 3763.

(12) (a) Duff, D. G.; Baiker, A.; Edwards, P. P. *J. Chem. Soc., Chem. Commun.* **1993**, 96. (b) Kulkarni, G. U.; Aiyer, H. N.; Vijayakrishnan, V.; Arunarkavalli, T.; Rao, C. N. R. *J. Chem. Soc., Chem. Commun.* **1993**, 1545.

(13) (a) Vijayakrishnan, V.; Rao, C. N. R. *Surf. Sci. Lett.* **1991**, *255*, L516. (b) Vijayakrishnan, V.; Chainani, A.; Sarma, D. D.; Rao, C. N. R. *J. Phys. Chem.* **1992**, *96*, 8679.

(14) Rao, C. N. R.; Vijayakrishnan, V.; Aiyer, H. N.; Kulkarni, G. U.; Subbanna, G. N. *J. Phys. Chem.* **1993**, *97*, 11157.

(15) Laibinis, P. E.; Whitesides, G. M.; Allara, D. L.; Tao, Y. T.; Parikh, A. N.; Nuzzo, R. G. *J. Am. Chem. Soc.* **1991**, *113*, 7152.